

1 **Phage mobility is a core determinant of phage-bacteria**  
2 **coexistence in biofilms**

3

4 Running title: Phage diffusion in bacterial biofilms

5

6

7 Matthew Simmons<sup>1</sup>, Knut Drescher<sup>2,3</sup>, Carey D. Nadell<sup>2,4\*†</sup>, Vanni Bucci<sup>1\*†</sup>

8

9

10 <sup>1</sup> Department of Biology, Program in Biotechnology and Biomedical Engineering, University of  
11 Massachusetts Dartmouth, N. Dartmouth, MA 02747, USA

12

13 <sup>2</sup> Max Planck Institute for Terrestrial Microbiology, D-35043 Marburg, Germany

14

15 <sup>3</sup> Department of Physics, Philipps University Marburg, D-35032 Marburg, Germany

16

17 <sup>4</sup> Department of Biological Sciences, Dartmouth College, Hanover, NH 03755, USA

18

19 The authors declare that they have no conflicts of interest

20

21 \* **Equal contribution**

22

23 † **Correspondence to:** [carey.d.nadell@dartmouth.edu](mailto:carey.d.nadell@dartmouth.edu), [vanni.bucci@umassd.edu](mailto:vanni.bucci@umassd.edu)

24 **Abstract**

25 Many bacteria are adapted for attaching to surfaces and for building complex communities,  
26 termed biofilms. The biofilm mode of life is predominant in bacterial ecology. So, too, is  
27 exposure of bacteria to ubiquitous viral pathogens, termed bacteriophages. Although biofilm-  
28 phage encounters are likely to be very common in nature, little is known about how phages  
29 might interact with biofilm-dwelling bacteria. It is also unclear how the ecological dynamics of  
30 phages and their hosts depend on the biological and physical properties of the biofilm  
31 environment. To make headway in this area, here we develop the first biofilm simulation  
32 framework that captures key mechanistic features of biofilm growth and phage infection. Using  
33 these simulations, we find that the equilibrium state of interaction between biofilms and phages  
34 is governed largely by nutrient availability to biofilms, infection likelihood per host encounter,  
35 and the ability of phages to diffuse through biofilm populations. Interactions between the biofilm  
36 matrix and phage particles are thus likely to be of fundamental importance, controlling the extent  
37 to which bacteria and phages can coexist in natural contexts. Our results open avenues to new  
38 questions of host-parasite coevolution and horizontal gene transfer in spatially structured biofilm  
39 contexts.

40

41

42

43 **Keywords**

44 biofilm, phage, phage mobility, diffusion limitation, matrix, host-parasite, simulation, spatial  
45 structure

## 46 Introduction

47 Bacteriophages, the viral parasites of bacteria, are predominant agents of bacterial death and  
48 horizontal gene transfer in nature (Suttle 2007, Thomas and Nielsen 2005). Their ecological  
49 importance and relative ease of culture in the lab have made bacteria and their phages a  
50 centerpiece of classical and recent studies of molecular genetics (Cairns et al 2007, Labrie et  
51 al 2010, Salmond and Fineran 2015, Samson et al 2013, Susskind and Botstein 1978) and host-  
52 parasite interaction (Bohannan and Lenski 2000, Brockhurst et al 2005, Chao et al 1977, Forde  
53 et al 2004, Gomez and Buckling 2013, Gómez and Buckling 2011, Kerr et al 2006, Koskella and  
54 Brockhurst 2014, Lenski and Levin 1985, Levin et al 1977, Vos et al 2009). This is a venerable  
55 literature with many landmark discoveries, most of which have focused on liquid culture  
56 conditions. In addition to living in the planktonic phase, many microbes are adapted for  
57 interacting with surfaces, attaching to them, and forming multicellular communities (Meyer et al  
58 2012, Nadell et al 2016, O'Toole and Wong 2016, Persat et al 2015, Teschler et al 2015, van  
59 Vliet and Ackermann 2015, Weitz et al 2005). These communities, termed biofilms, are  
60 characteristically embedded in an extracellular matrix of proteins, DNA, and sugar polymers  
61 that play a large role in how the community interacts with the surrounding environment (Dragoš  
62 and Kovács 2017, Flemming and Wingender 2010).

63 Since growth in biofilms and exposure to phages are common features of bacterial life,  
64 we can expect biofilm-phage encounters to be fundamental to microbial natural history (Abedon  
65 2008, Abedon 2012, Díaz-Muñoz and Koskella 2014, Koskella et al 2011, Koskella 2013, Nanda  
66 et al 2015). Furthermore, using phages to kill unwanted bacteria – which was eclipsed in 1940  
67 by the advent of antibiotics in Western medicine – has experienced a revival in recent years as  
68 an alternative antimicrobial strategy (Azeredo and Sutherland 2008, Chan et al 2013, Levin and  
69 Bull 2004, Melo et al 2014, Pires et al 2011, Sillankorva et al 2010). Understanding biofilm-  
70 phage interactions is thus an important new direction for molecular, ecological, and applied  
71 microbiology. Existing work suggests that phage particles may be trapped in the extracellular  
72 matrix of biofilms (Briandet et al 2008, Doolittle et al 1996, Lacroix-Gueu et al 2005); other  
73 studies have used macroscopic staining assays to measure changes in biofilm size before and  
74 after phage exposure, with results ranging from biofilm death, to no effect, to biofilm  
75 augmentation (reviewed by (Chan and Abedon 2015)). There is currently only a very limited  
76 understanding of the mechanisms responsible for this observed variation in outcome, and there  
77 has been no systematic exploration of how phage infections spread within living biofilms on the  
78 length scales of bacterial cells.

79 Biofilms, even when derived from a single clone, are heterogeneous in space and time  
80 (Ackermann 2015, Stewart and Franklin 2008). The extracellular matrix can immobilize a large  
81 fraction of cells, constraining their movement and the mass transport of soluble nutrients and  
82 wastes (Flemming and Wingender 2010, Teschler et al 2015). Population spatial structure, in  
83 turn, has a fundamental impact on intra- and inter-specific interaction patterns (Durrett and Levin  
84 1994, Kovács 2014, Nadell et al 2016). Theory predicts qualitative changes in population  
85 dynamics when host-parasite contact rate is not a simple linear function of host and parasite  
86 abundance (Liu et al 1986), which is almost certainly the case for phages and biofilm-dwelling  
87 bacteria under spatial constraint. It is thus very likely that the interaction of bacteria and phages  
88 will be altered in biofilms relative to mixed or stationary liquid environments. Available literature  
89 supports the possibility of altered phage population dynamics in biofilms (Ashby et al 2014,  
90 Gómez and Buckling 2011, Heilmann et al 2012, Scanlan and Buckling 2012, Vos et al 2009),  
91 but the underlying details of the phage-bacterial interactions have been difficult to access  
92 experimentally or theoretically. Spatial simulations that capture core mechanistic features of  
93 biofilms are a promising avenue to begin tackling this problem. Here, we use a simulation  
94 approach to study how the biofilm environment can influence micrometer-scale population  
95 dynamics of bacteria and phages, highlighting connections between this research area and  
96 classical findings from spatial disease ecology.

97 Existing biofilm simulation frameworks are flexible and have excellent experimental  
98 support (Bucci et al 2011, Estrela et al 2012, Estrela and Brown 2013, Hellweger and Bucci  
99 2009, Hellweger et al 2016, Lardon et al 2011, Nadell et al 2016, Naylor et al 2017), but they  
100 become impractical when applied to the problem of phage infection. We therefore developed a  
101 new simulation framework to study phage-biofilm interactions. Using this approach, we find that

102 nutrient availability and phage infection rates are critical control parameters of phage spread;  
103 furthermore, modest changes in the diffusivity of phages within biofilms can cause qualitative  
104 shifts toward stable or unstable coexistence of phages and biofilm-dwelling bacteria. The latter  
105 result implies a central role for the biofilm extracellular matrix in phage ecology.  
106

107

## 108 **Methods**

109 When phages are implemented as discrete individuals, millions of independent agents can be  
110 active in a single simulation space on the order of several hundred bacterial cell lengths.  
111 Moreover, the time scale for calculating bacterial growth can be an order of magnitude larger  
112 than the appropriate time scale for phage replication and diffusion. These problems create  
113 unmanageable computational load for tracking large population sizes when bacteria and  
114 phages are modeled in continuous space, as is the case for contemporary biofilm simulations,  
115 which are not designed to accommodate these obstacles (Lardon et al 2011). We therefore  
116 developed a new framework customized for studying biofilm-phage interactions. To solve these  
117 issues, we reduced the amount of spatial detail with which cells are implemented, using a grid-  
118 based approach for bacterial biomass calculation. Within each grid node bacteria are  
119 considered well-mixed, and their biomass is converted to bacterial cell counts for infection  
120 calculations. We also estimate phage Brownian motion by calculating the analytical solution of  
121 the diffusion equation and using it as a distribution of the likelihood of finding each phage at  
122 each location, thus eliminating the need for calculating each phage's movement separately. Our  
123 model combines (i) a numerical solution of partial differential equations to determine solute  
124 concentrations in space, (ii) a cellular automaton method for simulating biofilms containing a  
125 user-defined, arbitrary number of bacterial strains with potentially different properties, and (iii)  
126 an agent-based method for simulating diffusible phages (Figure 1).

127 In each run, the simulation space (250  $\mu\text{m}$  x 250  $\mu\text{m}$ , with lateral periodic boundary  
128 conditions) is initiated with cells that are randomly distributed across the basal surface. The  
129 following steps are iterated until an exit steady-state criterion is met:

- 130 – Compute nutrient concentration profiles
- 131 – Compute bacterial biomass dynamics
- 132 – Redistribute biomass according to cellular automaton rules (i.e., cell shoving)
- 133 – Evaluate host cell lysis and phage propagation
- 134 – Simulate phage diffusion to determine new distribution of phage particles
- 135 – Assessment of match to exit criteria:

136 **Coexistence:** simulations reach a pre-defined end time with both bacteria and  
137 phages still present (these cases are re-assessed for long-term stability);

138 **Biofilm death:** the bacterial population declines to zero; or

139 **Phage extinction:** no phages or infected biomass remain in the biofilm.  
140

141 As in previous biofilm simulation frameworks, bacteria grow and divide according to local  
142 nutrient concentrations, which are calculated to account for diffusion from a bulk nutrient supply  
143 (above the biofilm, motivated by flow chamber biofilm culture systems) and absorption by  
144 bacteria. Specifically, when nutrients are abundant, most cells in the biofilm can grow. When  
145 nutrients are scarce, they are depleted by cells on the outermost layers of the biofilm, and  
146 bacteria in the interior stop growing. Cells on the exterior can be eroded due to shear (Alpkvist  
147 and Klapper 2007, Chambliss and Stewart 2007, Drescher et al 2013, Stewart 2012).  
148 Implementing biomass removal by shear is critical in allowing us to study the steady states of  
149 the system: without shear-induced sloughing, one is restricted to examining transient biofilm  
150 states (Bohn et al 2007, Bucci et al 2011). Sloughing is also required for implementing loss of  
151 biomass when phage infections destroy biofilms with rough surface fronts (see below). Bacterial  
152 growth, decay, and shear are implemented according to experimentally supported precedents  
153 in the literature (Bohn et al 2007, Xavier et al 2004, Xavier et al 2005a, Xavier et al 2005b).

154 Implementing phage infection, propagation, and diffusion is the primary innovation of  
155 the simulation framework we developed. To mimic phages that encounter a pre-grown biofilm  
156 after departing from a previous infection site, we performed our simulations such that biofilms  
157 could grow for a defined period, after which a single pulse of phages was introduced into the

158 system. During this pulse, lytic phages (Abedon 2008) are added to the simulation space all  
159 along the biofilm front. For every phage virion located in a grid node containing bacterial  
160 biomass, we calculate the probability of adsorption to a host cell, which is a function of the  
161 infection rate and the number of susceptible hosts in the grid node. Upon adsorption, the  
162 corresponding bacterial biomass is converted from uninfected to an infected state (Figure 1),  
163 and, following an incubation period, the host cell lyses and releases progeny phages with a  
164 defined burst size. In the primary analysis below, burst size is fixed at an empirically  
165 conservative number, but we also explore robustness of the results to variation in burst size in  
166 a supplementary analysis (see Results). Phages move within the biofilm and in the liquid  
167 medium by Brownian motion; the model analytically solves the diffusion equation of a Dirac  
168 delta function at each grid position to build a probability distribution from which to resample the  
169 phage locations.

170 As the pattern of phage diffusion is probably important for how phage-biofilm interactions  
171 occur, we devoted particular attention to building flexibility into the framework for this purpose.  
172 The diffusivity of phage particles is likely to decrease when they are embedded in biofilm matrix  
173 material, but to what extent phage diffusivity changes may vary from one case to another in  
174 natural settings. To study how phage movement inside biofilms influences phage infection  
175 dynamics, we introduce a parameter,  $Z_p$ , which we term phage impedance. For  $Z_p = 1$ , phage  
176 diffusivity is the same inside and outside of biofilms. As the value of  $Z_p$  is increased, phage  
177 diffusive movement inside biofilms is decreased relative to normal aqueous solution. Theory  
178 predicts that it will be easier for diffusing particles to enter a 3-dimensional mesh maze - which  
179 is a reasonable conceptualization of the biofilm matrix - than it is for the same particle to exit  
180 the mesh (McCrea and Whipple 1940, Motwani and Raghavan 1995). Our model of phage  
181 movement incorporates this predicted property of biofilm matrix material by making it easier for  
182 phages to cross from the surrounding liquid to the biofilm mass fraction than *vice versa* (see  
183 Supplementary Methods). We also explore the consequences of relaxing this assumption, such  
184 that phages can cross from the surrounding liquid to biofilm, and *vice versa*, with equal ease  
185 (see Results).

186 All model parameters, where possible, were set according to precedent in the  
187 experimental literature and biofilm simulation literature. There is no experimental system for  
188 which all parameters in the framework have been measured, but the key biological parameters  
189 used here are, where possible, identical to experimentally measured values for *Escherichia coli*  
190 and the lytic phage T7 (Supplementary Table 1). Other key parameters were varied  
191 systematically to test for their effects on simulation outcomes (see Results).

192 To assess the core structure of our simulations, we compared the predictions obtained  
193 from a non-spatial version of the framework (i.e., using homogeneous nutrient, bacterial, and  
194 phage distributions) with results obtained from an ODE model incorporating the same processes  
195 and parameters as the simulations. These trials confirmed that the core population dynamics of  
196 the simulations perform according to expectation without spatial structure (see Supplementary  
197 Methods and Supplementary Figure S1). A detailed description of the simulation framework and  
198 explanation of its assumptions are provided in the Supplementary Methods. The framework  
199 code can be obtained from the Zenodo repository:  
200 <https://zenodo.org/record/268903#.WJho3bYrJHc>.

## 201 202 **Computation**

203 Our hybrid framework was written in the Python programming language, drawing from numerical  
204 methods developed in the literature (Bell et al 2011, Bresenham 1965, Dijkstra 1959). All  
205 data analysis was performed using the R programming language (see Supplementary  
206 Methods). Simulations were performed in parallel on the UMass Green High-Performance  
207 Computing Cluster. Each simulation requires 4-8 hours to execute, and more than 200,000  
208 simulations were performed for this study, totaling over 100 CPU-years of run time.

## 209 210 **Results**

211 The primary features distinguishing biofilm populations from planktonic populations are spatial  
212 constraint and heterogeneity in the distribution of solutes and cellular physiological state, which

213 includes growth rate, and – we hypothesize – phage infection. Our aim here is to identify how  
214 these features qualitatively influence bacteria-phage population dynamics in biofilms. We omit  
215 the possibility of co-evolution, i.e., we do not consider the origin and maintenance of phage  
216 resistance among bacteria, or mutations that alter phage host-range. This simplification was  
217 made in order to focus clearly on the mechanisms and impacts of limited movement (of growth-  
218 limiting nutrients, bacteria, and phages) on bacteria-phage interaction. The foundation  
219 established in this way will be a starting point for understanding the broader problem of eco-  
220 evolutionary interplay between phages and their hosts in biofilms.

221 We began by exploring the different possible outcomes of phage infection in biofilms as  
222 a function of phage infectivity, before moving on to a more systematic study of phage transport,  
223 phage infection, and bacterial growth rates.

224

## 225 **(a) Stable states of bacteria and phages in biofilms**

226 Intuitively, the population dynamics of bacteria and lytic phages should depend on the relative  
227 strength of bacterial growth and bacterial removal, including erosion and cell death caused by  
228 phage infection. We studied the behavior of the simulations by varying the relative magnitude  
229 of bacterial growth versus phage proliferation. In this manner, we could observe three broad  
230 stable state classes in the bacteria/phage population dynamics (Figure 2). We summarize these  
231 classes here before proceeding to a more systematic characterization of the simulation  
232 parameter space in the following section.

233

### 234 *(i) Biofilm death*

235 If phage infection and proliferation sufficiently out-pace bacterial growth, then the bacterial  
236 population eventually declines to zero as it is consumed by phages and erosion (Figure 2A).  
237 Phage infections progressed in a relatively homogeneous wave, if host biofilms were flat  
238 (Supplementary Video SV1). For biofilms with uneven surface topography, phage infections  
239 proceeded tangentially to the biofilm surface and "pinched off" areas of bacterial biomass, which  
240 were then sloughed away after losing their connection to the remainder of the biofilm  
241 (Supplementary Video SV2). This sloughing process eventually eliminated the bacterial  
242 population from the surface.

243

### 244 *(ii) Coexistence*

245 In some instances, both bacteria and phages remained present for the entire simulation run  
246 time. We found that coexistence could occur in different ways, most commonly with rounded  
247 biofilm clusters that were maintained by a balance of bacterial growth and death on their  
248 periphery (Supplementary Video SV3). When phage infection rate and nutrient availability were  
249 high, biofilms entered cycles in which tower structures were pinched off from the rest of the  
250 population by phage propagation, and from the remaining biofilm, new tower structures re-grew  
251 and were again partially removed by phages (Figure 2B, Supplementary Video SV4). We  
252 confirmed the stability of these coexistence outcomes by running simulations for extended  
253 periods of time, varying initial conditions and the timing of phage exposure to ensure that host  
254 and phage population sizes either approached constant values or entrained in oscillation  
255 regimes (see below).

256

### 257 *(iii) Phage extinction*

258 We observed many cases in which phages either failed to establish a spreading infection, or  
259 declined to extinction after briefly propagating in the biofilm (Figure 2C). This occurred when  
260 phage infection probability was low, but also, less intuitively, when nutrient availability and thus  
261 bacterial growth were very low, irrespective of infection probability. Visual inspection of the  
262 simulations showed that when biofilms were sparse and slow-growing, newly released phages  
263 were more likely to be swept away into the liquid phase than to encounter new host cells to  
264 infect (Supplementary Video SV5). At a conservative maximum bacterial growth rate, biofilms  
265 were not able to out-grow a phage infection. However, if bacterial growth was increased beyond  
266 this conservative maximum, we found that biofilms could effectively expel phage infections by  
267 shedding phages into the liquid phase above them (Supplementary Video SV6). This result, and

268 those described above, heavily depended on the ability of phages to diffuse through the biofilms,  
269 to which we turn our attention in the following section.

270

### 271 **(b) Governing parameters of phage spread in biofilms**

272 Many processes can contribute to the balance of bacterial growth and phage propagation in a  
273 biofilm. To probe our simulation framework systematically, we used our pilot simulations to  
274 choose control parameters with strong influence on the outcome of phage-host population  
275 dynamics. We then performed sweeps of parameter space to build up a general picture of how  
276 the population dynamics of the biofilm-phage system depends on underlying features of  
277 phages, host bacteria, and biofilm spatial structure.

278 We isolated three key parameters with major effects on how phage infections spread  
279 through biofilms. The first of these is environmental nutrient concentration,  $N_{\max}$ , an important  
280 ecological factor that heavily influences biofilm growth and architecture (Drescher et al 2016,  
281 Nadell et al 2010). Importantly, varying  $N_{\max}$  not only changes the overall growth rate but also  
282 the emergent biofilm spatial structure. When nutrients are sparse, for example, biofilms grow  
283 with tower-like projections and high variance in surface height (Picioreanu et al 1998), whereas  
284 when nutrients are abundant, biofilms tend to grow with smooth fronts and low variance in  
285 surface height (Nadell et al 2010, Nadell et al 2013, Picioreanu et al 1998). We computationally  
286 swept  $N_{\max}$  values to vary biofilm growth from near zero to a conservative maximum allowing  
287 for biofilm growth to a height of 250  $\mu\text{m}$  in 24 hours without phage exposure. The second  
288 governing parameter is phage infection probability, which we varied from 0.1% to 99% per  
289 phage-host encounter. Phage burst size is also important, but above a threshold value  
290 (approximately 100 new phages per lysed host), we found that its qualitative influence on our  
291 results saturated (Supplementary Figure S2). Lower burst sizes exerted similar effects to  
292 lowering the probability of phage infection per host encounter. For simplicity in the rest of the  
293 paper, we use a fixed burst size of 100, which is typical for model lytic phages such as T7 (Endy  
294 et al 2000).

295 Our pilot simulations with the framework suggested that a third factor, the relative  
296 diffusivity of phages within biofilms, may be fundamental to phage-bacteria population  
297 dynamics. We therefore varied phage movement within the biofilm by changing the phage  
298 impedance parameter  $Z_p$ ; larger values of  $Z_p$  correspond to slower phage diffusivity within  
299 biofilms relative to the surrounding liquid.

300 We performed thousands of simulations in parallel to study the influence of nutrients,  
301 infection probability, and phage mobility on population dynamics. In Figure 3, the results are  
302 visualized as sweeps of nutrient concentration versus phage infectivity for three values of phage  
303 impedance. For each combination of these three parameters, we show the distribution of  
304 simulation exit conditions, including biofilm death, phage extinction, or phage-bacteria  
305 coexistence. In some cases, biofilms grew to the ceiling of the simulation space, such that the  
306 biofilm front could no longer be simulated accurately. To be conservative, the outcome of these  
307 cases was designated as “undetermined”, but they likely correspond to phage extinction or  
308 coexistence.

309 We first considered the extreme case in which phage diffusion is unaltered inside  
310 biofilms (phage impedance value of  $Z_p = 1$ ). In these conditions, coexistence does not occur,  
311 and bacterial populations do not survive phage exposure unless infection probability is nearly  
312 zero, or if nutrient availability is so low that little bacterial growth is possible (Figure 3A). In these  
313 latter cases, as we described above, phages either cannot establish an infection at all or are  
314 unlikely to encounter new hosts after departing from an infected host after it bursts. Bacterial  
315 survival in this regime depends on the spatial structure of biofilm growth, including the  
316 assumption that phages which have diffused away from the biofilm surface are advected out of  
317 the system. Importantly, using the same experimentally constrained parameters for bacteria  
318 and phages, but in a spatially homogenized version of the framework – which approximates a  
319 mixed liquid condition – elimination of the bacterial population was the only outcome  
320 (Supplementary Figure S1). This comparison further highlights the importance of spatial effects  
321 on this system’s population dynamics.

322 When phage diffusivity is reduced within biofilms relative to the surrounding liquid  
323 (phage impedance value of  $Z_p = 10$ ), biofilm-dwelling bacteria survive infection for a wider range

324 of phage infection probability (Figure 3B). Phages and host bacteria coexist with each other at  
325 low to moderate infection probability and high nutrient availability for bacterial growth. Within  
326 this region of coexistence, we could find cases where phage and host populations converge to  
327 stable fixed equilibria, and others in which bacterial and phage populations enter stable  
328 oscillations. The former corresponds to stationary biofilm clusters with a balance of bacterial  
329 growth and phage proliferation on their periphery (as in Supplementary Video SV3), while the  
330 latter corresponds to cycles of biofilm tower projection growth and sloughing after phage  
331 proliferation (as in Supplementary Video SV4). For low nutrient availability, slow-growing  
332 biofilms could avoid phage epidemics by providing too few host cells for continuing infection.

333 As phage diffusivity within biofilms is decreased further (Figure 3C), coexistence occurs  
334 for a broader range of nutrient and infectivity conditions, and biofilm-dwelling bacteria are more  
335 likely to survive phage exposure. Interestingly, for  $Z_P = 15$  there was a substantial expansion of  
336 the parameter range in which biofilms survive and phages go extinct. For  $Z_P = 10$  and  $Z_P = 15$ ,  
337 we also found cases of unstable coexistence in which bacteria and phages persisted together  
338 transiently, but then either the host or the phage population declined to extinction stochastically  
339 over time (Figure 3D-E). Depending on the relative magnitudes of bacterial growth (low vs. high  
340 nutrients) and phage infection rates, this unstable coexistence regime was shifted toward biofilm  
341 survival or elimination.

342 Overall, the tendency of the system toward different stable states in parameter space  
343 could be shifted by modest changes in any of the key parameters tested. For example, in Figure  
344 3C, at intermediate phage infectivity, low nutrient availability resulted in biofilm survival.  
345 Increasing nutrient input leads to biofilm death as biofilms become large enough for phages to  
346 take hold and spread through the population. Further increasing nutrient availability leads to a  
347 region of predominant coexistence as higher bacterial growth compensates for phage-mediated  
348 death. And, finally, increasing nutrient input further still leads to stochastic outcomes of biofilm  
349 survival and biofilm death, with the degree of biofilm sloughing and erosion imposing chance  
350 effects on whether biofilms survive phage exposure.

351 The stochasticity inherent to the spatial simulations provides an inherent test of stability  
352 to small perturbations. To assess the broader robustness of our results to initial conditions, we  
353 repeated the parameter sweeps, but varied the time at which phages were introduced to the  
354 system. We found that the outcomes were qualitatively identical when compared with the data  
355 described above (Supplementary Figure S3). Our main analysis in Figure 3 also assumes that  
356 key biological parameters are held at one fixed value in the bacterial and phage populations  
357 within any single simulation. This is a simplification relative to natural systems (Hellweger and  
358 Bucci 2009), in which these parameters may vary from one bacterium and phage virion to  
359 another. If this simplifying assumption is relaxed, and maximum bacterial growth rate, phage  
360 infectivity, phage burst size, and phage latent period are normally distributed in each simulation  
361 run, we again observed qualitatively identical results (Supplementary Figure S4).

362  
363 **(c) Population stable states as a function of phage diffusivity**  
364 The findings summarized in Figure 3 suggest that phage diffusivity (reflected by the phage  
365 impedance  $Z_P$ ) is a critical parameter controlling population dynamics in biofilms. We assessed  
366 this idea systemically by varying phage impedance at high resolution and determining the  
367 effects on phage/bacteria stable states spectra. For each value of phage impedance ( $Z_P = 1 -$   
368  $18$ ), we performed parameter sweeps for the same range of nutrient availability and phage  
369 infection probability as described in the previous section, and quantified the fraction of  
370 simulations resulting in biofilm death, phage-bacteria coexistence, and phage extinction (Figure  
371 4). With increasing  $Z_P$  we found an increase in the fraction of simulations ending in long-term  
372 biofilm survival, either through phage extinction or coexistence. We expected the parameter  
373 space in which phages eliminate biofilms to contract to nil as phage impedance was increased.  
374 However, this was not the case; the stable states distribution, which saturated at approximately  
375  $Z_P = 15$ , always presented a fraction of simulations in which bacteria were eliminated by phages.  
376 This result depended to a degree on the symmetry of phage diffusion across the interface of  
377 the biofilm and the surrounding liquid. As noted in the Methods section, theory predicts that  
378 phages can enter the biofilm matrix mesh more easily than they can exit, and this is the default  
379 mode of our simulations (McCrea and Whipple 1940, Motwani and Raghavan 1995). If, on the



380 other hand, phages can diffuse across the biofilm boundary back into the liquid just as easily as  
381 they can cross from the liquid to the biofilm, then as  $Z_P$  increases, then biofilm death occurs less  
382 often, and bacteria-phage coexistence becomes more predominant (Supplementary Figure S5).

383  
384

## 385 Discussion

386 Biofilm-phage interactions are likely to be ubiquitous in the natural environment and,  
387 increasingly, phages are drawing attention as the basis for new antibacterial strategies (Abedon  
388 2015). Due to the complexity of the spatial interplay between bacteria and their phages in the  
389 biofilm context, simulations and mathematical modeling serve a critical role for identifying and  
390 understanding important features of phage-biofilm interactions. Across species and contexts,  
391 biofilms are defined by the spatial constraint, altered diffusion environment, and heterogeneous  
392 solute distribution conditions created by cells while embedded in an extracellular matrix. Here  
393 we developed a new simulation framework that captures these essential processes, and used  
394 it to study how they alter the population dynamics of susceptible bacteria and lytic phages.

395 At the outset of this study, we hypothesized that bacteria might be able to survive phage  
396 attack when nutrients are abundant and bacterial growth rate is high. The underlying rationale  
397 was that if bacterial growth and biofilm erosion are fast enough relative to phage proliferation,  
398 then biofilms could simply shed phage infections from their outer surface into the passing liquid.  
399 This result was not obtained, even when nutrient influx and thus bacterial growth were  
400 conservatively high. We speculate that for biofilms to shed phage infections in this manner,  
401 phage incubation must be long relative to bacterial growth, and/or biofilm erosion must be  
402 exceptionally strong, such that biomass on the biofilm exterior is rapidly and continuously lost  
403 into the liquid phase. Our results do not eliminate this possibility entirely, but they suggest that  
404 this kind of spatial escape from phage infection does not occur under a broad range of  
405 conditions.

406 Biofilms could repel phage attack in our simulations when nutrient availability was low,  
407 resulting in slow bacterial growth and widely spaced biofilm clusters. When biofilms are sparse,  
408 phage-bacteria encounters are less likely to occur, and thus a higher probability of infection per  
409 phage-host contact event is required to establish a phage epidemic. Even if phages do establish  
410 an infection, when bacterial growth rates are low, the nearest biofilm cluster may be far enough  
411 away from the infected cell group that phages simply are not able to spread from one biofilm  
412 cluster to another before being swept away by fluid flow. Note that this observation likely  
413 depends on the scale of observation (Levin 1992): in a meta-population context, phage  
414 proliferation and subsequent removal into the passing liquid may lead to an epidemic on a larger  
415 spatial scale. This caveat aside, our findings are directly analogous to the concept of threshold  
416 host density as it applies in wildlife disease ecology (Boots and Sasaki 2002, Holt et al 2003,  
417 Keeling 1999, Lloyd-Smith et al 2005, May and Anderson 1979, Maynard-Smith 1974, Rand et  
418 al 1995, Satō et al 1994, Webb et al 2007). If host organisms, or clusters of hosts, are not  
419 distributed densely enough relative to the production rate and dispersal of a parasite, then  
420 epidemics cannot be sustained. Our spatial simulations, which implement the essential biofilm-  
421 specific mechanics of bacterial growth and phage infection, can thus recapitulate qualitative  
422 features of classical work in spatial epidemiology. This outcome draws concrete links between  
423 the microscopic world of phage-host population dynamics and the macroscopic world of disease  
424 spread, with results expressed in terms of parameters that are experimentally accessible to  
425 microbiologists. We hope that these key concepts may be used in the future as a bridge between  
426 researchers studying spatial disease ecology, bacterial biofilms, and bacteriophages.

427 Our results suggest that coexistence of lytic phages and susceptible host bacteria will  
428 occur more readily as phage diffusivity decreases within biofilms, but this outcome also depends  
429 strongly on phage infectivity and nutrient flux. In two important modeling studies on phage-  
430 bacteria interactions under spatial constraint, Heilmann et al. concluded that coexistence can  
431 occur under a broad array of conditions if bacteria are provided with refuges, that is, areas in  
432 which phage infectivity is decreased (Heilmann et al 2010, Heilmann et al 2012). An important  
433 distinction of our approach is that bacterial refuges against phage infection emerge  
434 spontaneously because of the interaction between spatial constraint, biofilm growth, phage

435 proliferation/diffusion, and erosion of bacterial biomass into the surrounding liquid phase.  
436 Coexistence of bacteria and phages can be rendered dynamically unstable by modest changes  
437 in nutrient availability, phage infectivity, or phage diffusion. In other words, spatial structure is  
438 not enough to guarantee phage/bacteria coexistence; rather, given that bacteria and phages  
439 are spatially constrained, one must also understand the total balance of biofilm expansion,  
440 biofilm erosion, phage infectivity, and phage advection/diffusion in order to understand the  
441 system's population dynamics.

442 The extracellular matrix is central to the ecology and physiology of biofilms (Branda et  
443 al 2005, Dragoš and Kovács 2017, Flemming and Wingender 2010, Flemming et al 2016, Nadell  
444 et al 2009, Nadell et al 2015, Nadell et al 2016, Teschler et al 2015). In the simulations explored  
445 here, biofilm matrix was modeled implicitly and is assumed to cause changes in phage  
446 diffusivity; our results support the intuition that by altering phage mobility and phages' physical  
447 access to new hosts, the biofilm matrix is likely to be important in the ecological interplay of  
448 bacteria and their phages (Abedon 2017). A crucial role for the matrix in phage-bacteria  
449 interactions is also supported by the common observation that matrix-degrading enzymes are  
450 encoded on phage genomes, which indicates that reducing the matrix diffusion barrier is an  
451 important fitness currency for phages in natural environments (Chan and Abedon 2015, Pires  
452 et al 2016).

453 Experiments comparing population dynamics of lytic phages and bacteria in well-mixed  
454 versus standing liquid cultures indicate that spatial heterogeneity can promote host-parasite  
455 coexistence (Brockhurst et al 2006). The biofilm environment shares some conceptual similarity  
456 to standing liquid cultures, but is qualitatively different in its details, including sharp gradients of  
457 nutrient availability and growth within biofilms, removal of cells from the biofilm system by  
458 dispersal, strong diffusion attenuation, and matrix-imposed spatial constraints. Our work lends  
459 support to an early suggestion that so-called wall populations on the inner surfaces of culture  
460 flasks can promote bacteria-phage coexistence (Schrag and Mittler 1996). The populations  
461 described in this work were, almost certainly, biofilms of matrix-embedded cells bound to the  
462 flask walls. The details by which this coexistence result occurs have not been clear; there is  
463 very little experimental work thus far on the spatial localization and diffusion of phages inside  
464 biofilms, but the limited available literature is consistent with the idea that the matrix alters phage  
465 movement (Briand et al 2008, Doolittle et al 1996, Sutherland et al 2004). In biofilms of *E. coli*,  
466 the matrix does indeed appear to reduce phage infection (May et al 2011), and recent work with  
467 biofilms of *Pseudomonas aeruginosa* grown in artificial sputum further supports the idea that  
468 matrix reduces phage susceptibility (Darch et al 2017). Experimental evolution approaches  
469 have shown that bacteria and their phages follow different evolutionary trajectories in biofilms  
470 versus planktonic culture (Davies et al 2016, Gómez and Buckling 2011, Scanlan and Buckling  
471 2012). Especially compelling in the context of this work, *P. fluorescens* evolves matrix hyper-  
472 production in response to consistent phage attack (Scanlan and Buckling 2012). Thinking about  
473 phage diffusion and biofilm population structuring will be important not just to the ecological  
474 community but also to molecular microbiologists trying to understand the mechanisms  
475 underlying phage transport through bacterial populations that are embedded in matrix material.

476 Here we have identified key properties of phages and their host cells that fundamentally  
477 impact population dynamics in bacterial biofilms. To achieve this, some elements of bacteria-  
478 phage interaction were not considered here. For instance, we have not implemented co-  
479 evolution, though phage and bacterial populations can co-evolve rapidly (Koskella and  
480 Brockhurst 2014, Levin and Bull 2004, Perry et al 2015, Thompson 1994, Weitz et al 2005).  
481 Selection imposed by phage-mediated killing is responsible for the evolution of diverse host  
482 defenses, including altered cell exterior structure, restriction endonucleases, sacrificial auto-  
483 lysis, and the CRISPR-Cas adaptive immune system (Labrie et al 2010). These host defense  
484 innovations have, in turn, spurred the evolution of sophisticated host attack strategies on the  
485 part of phages (Samson et al 2013). To break ground on the topic of phage-host population  
486 dynamics in heterogeneous biofilms, we have set aside the problem of coevolution here;  
487 coevolution is undoubtedly important, however, and we expect that biofilm environments will  
488 influence it strongly. For example, the typical population sizes of bacteria and phages, as well  
489 as their mutual encounter rates, may be dramatically different in biofilms containing tens of  
490 thousands of spatially constrained cells, relative to liquid cultures containing tens of billions of

491 well-mixed cells. The time scales and spatial patterns of bacteria-phage coevolution in biofilms  
492 may therefore differ substantially from those in liquid culture, which is an important area for  
493 future work. We have focused only on lytic phages, but understanding within-biofilm population  
494 dynamics of lysogenic phages, which integrate into the genome of infected hosts, often  
495 changing their phenotypes and mediating horizontal gene transfer, is also a crucial topic.  
496 Overall, we envision that studying bacteria-phage interactions under the unique constraints of  
497 biofilm environments will yield important extensions on many fronts of this classical area of  
498 microbial ecology.

## 500 **Competing Interests**

501 We have no competing interests.

## 503 **Author Contributions**

504 CDN and VB conceived the project; MS, VB, and CDN designed simulations; MS wrote and  
505 performed simulations; MS, CDN, VB, and KD analyzed data; CDN, VB, MS, and KD wrote the  
506 paper.

## 508 **Acknowledgements**

509 We are grateful to Ann Tate and Steve Abedon for comments on an earlier version of the  
510 manuscript. C.D.N. is supported by the Cystic Fibrosis Foundation (STANTO15RO), NIH grant  
511 P20-GM113132 to the Dartmouth BioMT COBRE, and a Burke Award from Dartmouth College.  
512 V.B. acknowledges support from the National Institute of Allergy and Infectious Disease (grant  
513 R15-AI112985-01A), and the National Science Foundation (grant 1458347). K.D. is supported  
514 by the Max Planck Society, the Human Frontier Science Program (CDA00084/2015-C), the  
515 Behrens Weise Foundation, and the European Research Council (716734).

## 517 **References**

- 518 Abedon S (2017). Phage "delay" toward enhancing bacterial escape from biofilms: a more  
519 comprehensive way of viewing resistance to bacteriophages. *AIMS Microbiology* **3**: 186-226.  
520  
521 Abedon ST (ed) (2008) *Bacteriophage Ecology: Population Growth, Evolution, and Impact of*  
522 *Bacterial Viruses*. Cambridge University Press: Cambridge, UK.  
523  
524 Abedon ST (2012). Spatial Vulnerability: Bacterial Arrangements, Microcolonies, and Biofilms  
525 as Responses to Low Rather than High Phage Densities. *Viruses-Basel* **4**: 663-687.  
526  
527 Abedon ST (2015). Ecology of anti-biofilm agents ii: bacteriophage exploitation and biocontrol  
528 of Biofilm Bacteria. *Pharmaceuticals* **8**: 559-589.  
529  
530 Ackermann M (2015). A functional perspective on phenotypic heterogeneity in microorganisms.  
531 *Nat Rev Microbiol* **13**: 497-508.  
532  
533 Alpkvist E, Klapper I (2007). Description of mechanical response including detachment using a  
534 novel particle model of biofilm/flow interaction. *Water Sci Technol* **55**: 265-273.  
535  
536 Ashby B, Gupta S, Buckling A (2014). Spatial Structure Mitigates Fitness Costs in Host-Parasite  
537 Coevolution. *The American Naturalist* **183**: E64-E74.  
538  
539 Azeredo J, Sutherland IW (2008). The use of phages for the removal of infectious biofilms.  
540 *Current Pharmaceutical Biotechnology* **9**: 261-266.  
541  
542 Bell W, Olsen L, Schroder J (2011). PyAMG: Algebraic multigrid solvers in Python v2.0,  
543 <http://www.pyamg.org>.  
544

- 545 Bohannan BJ, Lenski RE (2000). The relative importance of competition and predation varies  
546 with productivity in a model community. *The American Naturalist* **156**: 329-340.  
547
- 548 Bohn A, Zippel B, Almeida JS, Xavier JB (2007). Stochastic modeling for characterisation of  
549 biofilm development with discrete detachment events (sloughing). *Water Science and*  
550 *Technology* **55**: 257-264.  
551
- 552 Boots M, Sasaki A (2002). Parasite-driven extinction in spatially explicit host-parasite systems.  
553 *The American Naturalist* **159**: 706-713.  
554
- 555 Branda SS, Vik S, Friedman L, Kolter R (2005). Biofilms: the matrix revisited. *Trends Microbiol*  
556 **13**: 20-26.  
557
- 558 Bresenham JE (1965). Algorithm for computer control of a digital plotter. *IBM Systems journal*  
559 **4**: 25-30.  
560
- 561 Briandet R, Lacroix-Gueu P, Renault M, Lecart S, Meylheuc T, Bidnenko E *et al* (2008).  
562 Fluorescence correlation spectroscopy to study diffusion and reaction of bacteriophages inside  
563 biofilms. *Appl Environ Microb* **74**: 2135-2143.  
564
- 565 Brockhurst M, Buckling A, Rainey P (2006). Spatial heterogeneity and the stability of host-  
566 parasite coexistence. *J Evolution Biol* **19**: 374-379.  
567
- 568 Brockhurst MA, Buckling A, Rainey PB (2005). The effect of a bacteriophage on diversification  
569 of the opportunistic bacterial pathogen, *Pseudomonas aeruginosa*. *Proc R Soc B* **272**: 1385-  
570 1391.  
571
- 572 Bucci V, Nadell CD, Xavier JB (2011). The evolution of bacteriocin production in bacterial  
573 biofilms. *American Naturalist* **178**: E162-E173.  
574
- 575 Cairns J, Stent GS, Watson J (2007). *Phage and the Origins of Molecular Biology, Centennial*  
576 *Ed.*, 2 edn. Cold Spring Harbor Laboratory Press: Plainview, NY.  
577
- 578 Chambless JD, Stewart PS (2007). A three-dimensional computer model analysis of three  
579 hypothetical biofilm detachment mechanisms. *Biotechnol Bioeng* **97**: 1573-1584.  
580
- 581 Chan BK, Abedon ST, Loc-Carrillo C (2013). Phage cocktails and the future of phage therapy.  
582 *Future Microbiol* **8**: 769-783.  
583
- 584 Chan BK, Abedon ST (2015). Bacteriophages and their Enzymes in Biofilm Control. *Curr Pharm*  
585 *Des* **21**: 85-99.  
586
- 587 Chao L, Levin BR, Stewart FM (1977). A Complex Community in a Simple Habitat: An  
588 Experimental Study with Bacteria and Phage. *Ecology* **58**: 369-378.  
589
- 590 Darch SE, Kragh KN, Abbott EA, Bjarnsholt T, Bull JJ, Whiteley M (2017). Phage Inhibit  
591 Pathogen Dissemination by Targeting Bacterial Migrants in a Chronic Infection Model. *Mbio* **8**:  
592 e00240-00217.  
593
- 594 Davies EV, James CE, Williams D, O'Brien S, Fothergill JL, Haldenby S *et al* (2016). Temperate  
595 phages both mediate and drive adaptive evolution in pathogen biofilms. *Proceedings of the*  
596 *National Academy of Sciences* **113**: 8266-8271.  
597
- 598 Díaz-Muñoz SL, Koskella B (2014). Bacteria-phage interactions in natural environments. *Adv*  
599 *Appl Microbiol* **89**: 10.1016.  
600

- 601 Dijkstra EW (1959). A note on two problems in connexion with graphs. *Numerische mathematik*  
602 **1**: 269-271.  
603
- 604 Doolittle MM, Cooney JJ, Caldwell DE (1996). Tracing the interaction of bacteriophage with  
605 bacterial biofilms using fluorescent and chromogenic probes. *J Indust Microb* **16**: 331-341.  
606
- 607 Dragoš A, Kovács ÁT (2017). The Peculiar Functions of the Bacterial Extracellular Matrix.  
608 *Trends Microbiol.*  
609
- 610 Drescher K, Shen Y, Bassler BL, Stone HA (2013). Biofilm streamers cause catastrophic  
611 disruption of flow with consequences for environmental and medical systems. *Proceedings of*  
612 *the National Academy of Sciences* **110**: 4345-4350.  
613
- 614 Drescher K, Dunkel J, Nadell CD, van Teeffelen S, Grnja I, Wingreen NS *et al* (2016).  
615 Architectural transitions in *Vibrio cholerae* biofilms at single-cell resolution. *Proceedings of the*  
616 *National Academy of Sciences*: 201601702.  
617
- 618 Durrett R, Levin S (1994). The Importance of Being Discrete (and Spatial). *Theoretical*  
619 *Population Biology* **46**: 363-394.  
620
- 621 Endy D, You L, Yin J, Molineux IJ (2000). Computation, prediction, and experimental tests of  
622 fitness for bacteriophage T7 mutants with permuted genomes. *Proceedings of the National*  
623 *Academy of Sciences* **97**: 5375-5380.  
624
- 625 Estrela S, Trisos CH, Brown SP (2012). From metabolism to ecology: cross-feeding interactions  
626 shape the balance between polymicrobial conflict and mutualism. *The American naturalist* **180**:  
627 566-576.  
628
- 629 Estrela S, Brown SP (2013). Metabolic and Demographic Feedbacks Shape the Emergent  
630 Spatial Structure and Function of Microbial Communities. *PLoS Comput Biol* **9**: e1003398.  
631
- 632 Flemming H-C, Wingender J (2010). The biofilm matrix. *Nat Rev Microbiol* **8**: 623-633.  
633
- 634 Flemming H-C, Wingender J, Szewzyk U, Steinberg P, Rice SA, Kjelleberg S (2016). Biofilms:  
635 an emergent form of bacterial life. *Nat Rev Microbiol* **14**: 563-575.  
636
- 637 Forde SE, Thompson JN, Bohannan BJ (2004). Adaptation varies through space and time in a  
638 coevolving host–parasitoid interaction. *Nature* **431**: 841-844.  
639
- 640 Gomez P, Buckling A (2013). Coevolution with phages does not influence the evolution of  
641 bacterial mutation rates in soil. *ISME J* **7**: 2242-2244.  
642
- 643 Gómez P, Buckling A (2011). Bacteria-Phage Antagonistic Coevolution in Soil. *Science* **332**:  
644 106-109.  
645
- 646 Heilmann S, Sneppen K, Krishna S (2010). Sustainability of virulence in a phage-bacterial  
647 ecosystem. *Journal of virology* **84**: 3016-3022.  
648
- 649 Heilmann S, Sneppen K, Krishna S (2012). Coexistence of phage and bacteria on the boundary  
650 of self-organized refuges. *P Natl Acad Sci USA* **109**: 12828-12833.  
651
- 652 Hellweger FL, Bucci V (2009). A bunch of tiny individuals-Individual-based modeling for  
653 microbes. *Ecological Modelling* **220**: 8-22.  
654
- 655 Hellweger FL, Clegg RJ, Clark JR, Plugge CM, Kreft J-U (2016). Advancing microbial sciences  
656 by individual-based modelling. *Nat Rev Microbiol.*

657  
658 Holt RD, Dobson AP, Begon M, Bowers RG, Schaub EM (2003). Parasite establishment in  
659 host communities. *Ecology Letters* **6**: 837-842.  
660  
661 Keeling MJ (1999). The effects of local spatial structure on epidemiological invasions.  
662 *Proceedings of the Royal Society of London B: Biological Sciences* **266**: 859-867.  
663  
664 Kerr B, Neuhauser C, Bohannan BJM, Dean AM (2006). Local migration promotes competitive  
665 restraint in a host-pathogen 'tragedy of the commons'. *Nature* **442**: 75-78.  
666  
667 Koskella B, Thompson JN, Preston GM, Buckling A (2011). Local biotic environment shapes  
668 the spatial scale of bacteriophage adaptation to bacteria. *The American Naturalist* **177**: 440-  
669 451.  
670  
671 Koskella B (2013). Phage-mediated selection on microbiota of a long-lived host. *Curr Biol* **23**:  
672 1256-1260.  
673  
674 Koskella B, Brockhurst MA (2014). Bacteria–phage coevolution as a driver of ecological and  
675 evolutionary processes in microbial communities. *Fems Microbiol Rev* **38**: 916-931.  
676  
677 Kovács ÁT (2014). Impact of spatial distribution on the development of mutualism in microbes.  
678 *Frontiers in Microbiology* **5**: 649.  
679  
680 Labrie SJ, Samson JE, Moineau S (2010). Bacteriophage resistance mechanisms. *Nat Rev*  
681 *Micro* **8**: 317-327.  
682  
683 Lacroix-Gueu P, Briandet R, Leveque-Fort S, Bellon-Fontaine MN, Fontaine-Aupart MP (2005).  
684 In situ measurements of viral particles diffusion inside mucoid biofilms. *Comptes Rendus*  
685 *Biologies* **328**: 1065-1072.  
686  
687 Lardon LA, Merkey BV, Martins S, Doetsch A, Picioreanu C, Kreft J-U *et al* (2011). iDynoMiCS:  
688 next-generation individual-based modelling of biofilms. *Environ Microbiol* **13**: 2416-2434.  
689  
690 Lenski RE, Levin BR (1985). Constraints on the coevolution of bacteria and virulent phage: a  
691 model, some experiments, and predictions for natural communities. *American Naturalist*: 585-  
692 602.  
693  
694 Levin BR, Stewart FM, Chao L (1977). Resource-Limited Growth, Competition, and Predation:  
695 A Model and Experimental Studies with Bacteria and Bacteriophage. *The American Naturalist*  
696 **111**: 3-24.  
697  
698 Levin BR, Bull JJ (2004). Population and evolutionary dynamics of phage therapy. *Nat Rev*  
699 *Microbiol* **2**: 166-173.  
700  
701 Levin SA (1992). The Problem of Pattern and Scale in Ecology: The Robert H. MacArthur Award  
702 Lecture. *Ecology* **73**: 1943-1967.  
703  
704 Liu W-m, Levin SA, Iwasa Y (1986). Influence of nonlinear incidence rates upon the behavior  
705 of SIRS epidemiological models. *Journal of mathematical biology* **23**: 187-204.  
706  
707 Lloyd-Smith JO, Cross PC, Briggs CJ, Daugherty M, Getz WM, Latto J *et al* (2005). Should we  
708 expect population thresholds for wildlife disease? *Trends in Ecology & Evolution* **20**: 511-519.  
709  
710 May RM, Anderson RM (1979). Population biology of infectious diseases: Part II. *Nature* **280**:  
711 455-461.  
712

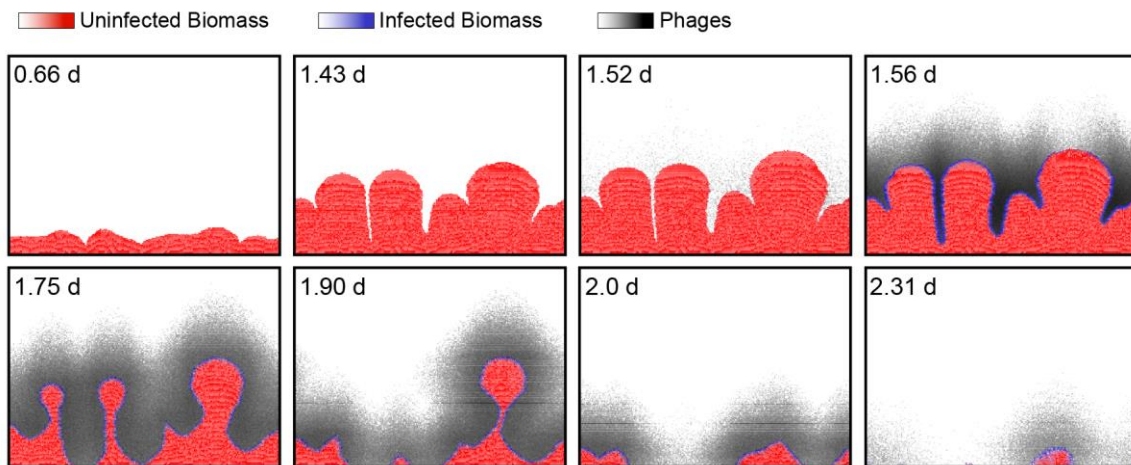
- 713 May T, Tsuruta K, Okabe S (2011). Exposure of conjugative plasmid carrying *Escherichia coli*  
714 biofilms to male-specific bacteriophages. *The ISME journal* **5**: 771.  
715
- 716 Maynard-Smith J (1974). *Models in ecology*. Cambridge University Press, Cambridge.  
717
- 718 McCrea W, Whipple F (1940). Random Paths in Two and Three Dimensions. *Proceedings of*  
719 *the Royal Society of Edinburgh* **60**: 281-298.  
720
- 721 Melo LDR, Sillankorva S, Ackermann H-W, Kropinski AM, Azeredo J, Cerca N (2014). Isolation  
722 and characterization of a new *Staphylococcus epidermidis* broad-spectrum bacteriophage.  
723 *Journal of General Virology* **95**: 506-515.  
724
- 725 Meyer JR, Dobias DT, Weitz JS, Barrick JE, Quick RT, Lenski RE (2012). Repeatability and  
726 Contingency in the Evolution of a Key Innovation in Phage Lambda. *Science* **335**: 428-432.  
727
- 728 Motwani R, Raghavan P (1995). *Randomized Algorithms*. Cambridge University Press:  
729 Cambridge, UK.  
730
- 731 Nadell CD, Xavier JB, Foster KR (2009). The sociobiology of biofilms. *Fems Microbiol Rev* **33**:  
732 206-224.  
733
- 734 Nadell CD, Foster KR, Xavier JB (2010). Emergence of spatial structure in cell groups and the  
735 evolution of cooperation. *PLoS Comput Biol* **6**: e1000716.  
736
- 737 Nadell CD, Bucci V, Drescher K, Levin SA, Bassler BL, Xavier JB (2013). Cutting through the  
738 complexity of cell collectives. *Proc R Soc B* **280**: 20122770.  
739
- 740 Nadell CD, Drescher K, Wingreen NS, Bassler BL (2015). Extracellular matrix structure governs  
741 invasion resistance in bacterial biofilms. *ISME J* **9**: 1700-1709.  
742
- 743 Nadell CD, Drescher K, Foster KR (2016). Spatial structure, cooperation, and competition in  
744 bacterial biofilms. *Nat Rev Microbiol* **14**: 589-600.  
745
- 746 Nanda AM, Thormann K, Frunzke J (2015). Impact of spontaneous prophage induction on the  
747 fitness of bacterial populations and host-microbe interactions. *J Bacteriol* **197**: 410-419.  
748
- 749 Naylor J, Fellermann H, Ding Y, Mohammed WK, Jakubovics NS, Mukherjee J *et al* (2017).  
750 Simbiotics: a multi-scale integrative platform for 3D modeling of bacterial populations. *ACS*  
751 *Synthetic Biology*.  
752
- 753 O'Toole GA, Wong GC (2016). Sensational biofilms: surface sensing in bacteria. *Curr Opin*  
754 *Microbiol* **30**: 139-146.  
755
- 756 Perry EB, Barrick JE, Bohannan BJM (2015). The Molecular and Genetic Basis of Repeatable  
757 Coevolution between *Escherichia coli* and Bacteriophage T3 in a Laboratory Microcosm. *PLoS*  
758 *ONE* **10**: e0130639.  
759
- 760 Persat A, Nadell C D, Kim M K, Ingremeau F, Siryaporn A, Drescher K *et al* (2015). The  
761 Mechanical World of Bacteria. *Cell* **161**: 988-997.  
762
- 763 Picioreanu C, van Loosdrecht MCM, Heijnen JJ (1998). Mathematical modeling of biofilm  
764 structure with a hybrid differential-discrete cellular automaton approach. *Biotechnology and*  
765 *Bioengineering* **58**: 101-116.  
766

- 767 Pires D, Sillankorva S, Faustino A, Azeredo J (2011). Use of newly isolated phages for control  
768 of *Pseudomonas aeruginosa* PAO1 and ATCC 10145 biofilms. *Research in Microbiology* **162**:  
769 798-806.  
770
- 771 Pires DP, Oliveira H, Melo LD, Sillankorva S, Azeredo J (2016). Bacteriophage-encoded  
772 depolymerases: their diversity and biotechnological applications. *Appl Microbiol Biotechnol* **100**:  
773 2141-2151.  
774
- 775 Rand D, Keeling M, Wilson H (1995). Invasion, stability and evolution to criticality in spatially  
776 extended, artificial host-pathogen ecologies. *Proceedings of the Royal Society of London B:*  
777 *Biological Sciences* **259**: 55-63.  
778
- 779 Salmond GPC, Fineran PC (2015). A century of the phage: past, present and future. *Nat Rev*  
780 *Micro* **13**: 777-786.  
781
- 782 Samson JE, Magadan AH, Sabri M, Moineau S (2013). Revenge of the phages: defeating  
783 bacterial defences. *Nat Rev Micro* **11**: 675-687.  
784
- 785 Satō K, Matsuda H, Sasaki A (1994). Pathogen invasion and host extinction in lattice structured  
786 populations. *Journal of mathematical biology* **32**: 251-268.  
787
- 788 Scanlan PD, Buckling A (2012). Co-evolution with lytic phage selects for the mucoid phenotype  
789 of *Pseudomonas fluorescens* SBW25. *ISME J* **6**: 1148-1158.  
790
- 791 Schrag SJ, Mittler JE (1996). Host-Parasite Coexistence: The Role of Spatial Refuges in  
792 Stabilizing Bacteria-Phage Interactions. *The American Naturalist* **148**: 348-377.  
793
- 794 Sillankorva S, Neubauer P, Azeredo J (2010). Phage control of dual species biofilms of  
795 *Pseudomonas fluorescens* and *Staphylococcus lentus*. *Biofouling* **26**: 567-575.  
796
- 797 Stewart PS, Franklin MJ (2008). Physiological heterogeneity in biofilms. *Nat Rev Microbiol* **6**:  
798 199-210.  
799
- 800 Stewart PS (2012). Mini-review: Convection around biofilms. *Biofouling* **28**: 187-198.  
801
- 802 Susskind MM, Botstein D (1978). Molecular genetics of bacteriophage P22. *Microbiological*  
803 *reviews* **42**: 385.  
804
- 805 Sutherland IW, Hughes KA, Skillman LC, Tait K (2004). The interaction of phage and biofilms.  
806 *Fems Microbiol Lett* **232**: 1-6.  
807
- 808 Suttle CA (2007). Marine viruses—major players in the global ecosystem. *Nat Rev Microbiol* **5**:  
809 801-812.  
810
- 811 Teschler JK, Zamorano-Sanchez D, Utada AS, Warner CJA, Wong GCL, Linington RG *et al*  
812 (2015). Living in the matrix: assembly and control of *Vibrio cholerae* biofilms. *Nat Rev Micro* **13**:  
813 255-268.  
814
- 815 Thomas CM, Nielsen KM (2005). Mechanisms of, and barriers to, horizontal gene transfer  
816 between bacteria. *Nature reviews Microbiology* **3**: 711.  
817
- 818 Thompson JN (1994). *The coevolutionary process*. University of Chicago Press.  
819
- 820 van Vliet S, Ackermann M (2015). Bacterial ventures into multicellularity: collectivism through  
821 individuality. *PLoS Biol* **13**: e1002162.  
822

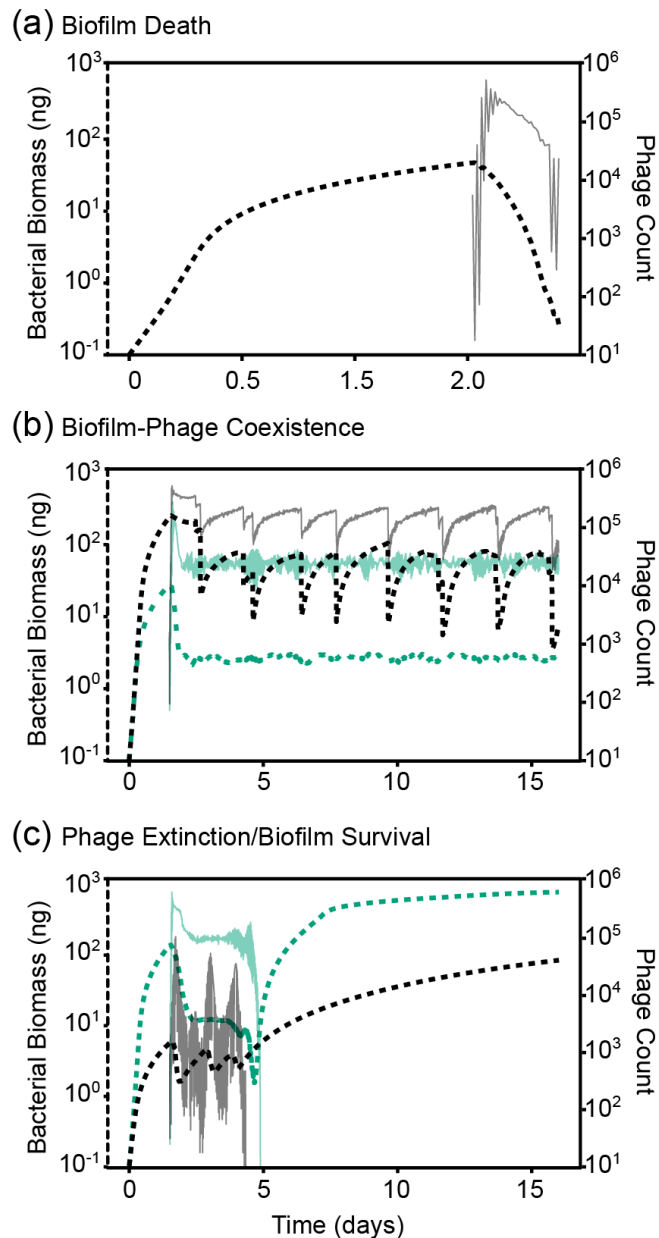


- 823 Vos M, Birkett PJ, Birch E, Griffiths RI, Buckling A (2009). Local Adaptation of Bacteriophages  
824 to Their Bacterial Hosts in Soil. *Science* **325**: 833.  
825
- 826 Webb SD, Keeling MJ, Boots M (2007). Host–parasite interactions between the local and the  
827 mean-field: How and when does spatial population structure matter? *J Theo Biol* **249**: 140-152.  
828
- 829 Weitz JS, Hartman H, Levin SA (2005). Coevolutionary arms races between bacteria and  
830 bacteriophage. *Proc Natl Acad Sci U S A* **102**: 9535-9540.  
831
- 832 Xavier JB, Picioreanu C, Van Loosdrecht MCM (2004). A modelling study of the activity and  
833 structure of biofilms in biological reactors. *Biofilms* **1**: 377-391.  
834
- 835 Xavier JB, Picioreanu C, Rani SA, van Loosdrecht MCM, Stewart PS (2005a). Biofilm-control  
836 strategies based on enzymic disruption of the extracellular polymeric substance matrix - a  
837 modelling study. *Microbiology-Sgm* **151**: 3817-3832.  
838
- 839 Xavier JB, Picioreanu C, van Loosdrecht M (2005b). A general description of detachment for  
840 multidimensional modelling of biofilms. *Biotechnology and Bioengineering* **91**: 651-669.  
841  
842  
843

844 **Figure Legends**  
845

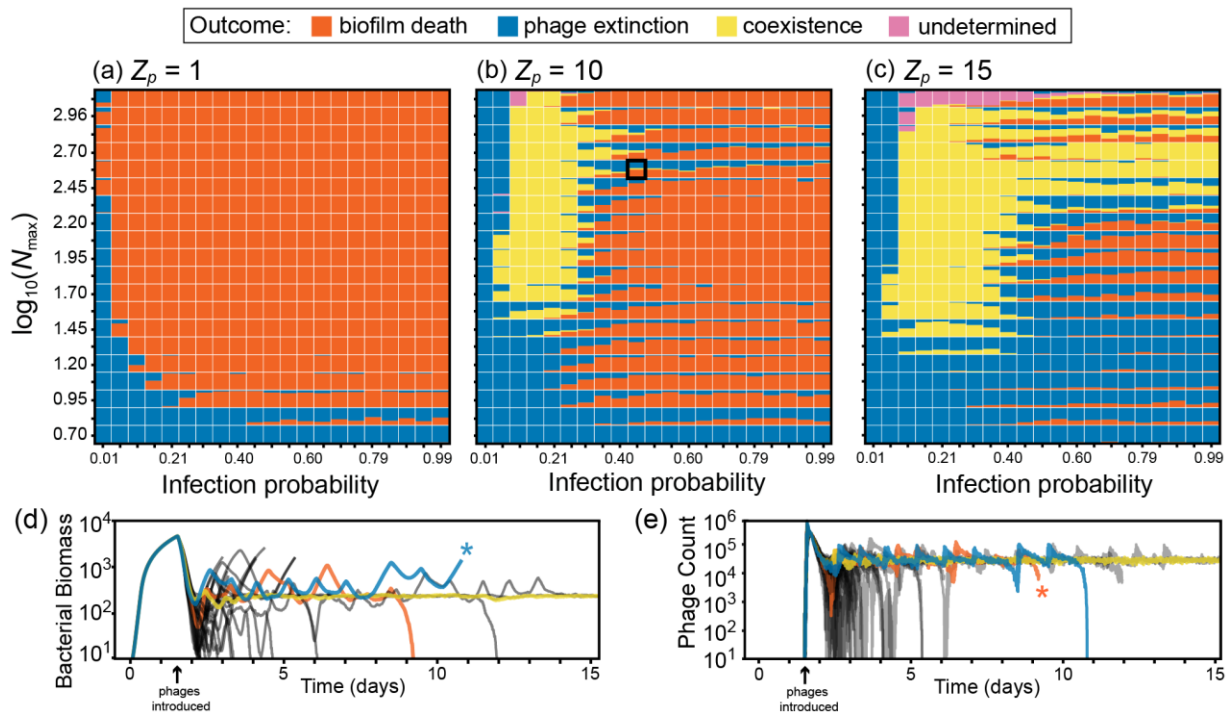


846 **Figure 1.** An example time series of simulated biofilm growth and phage infection. For  
847 uninfected and infected biomass (red and blue, respectively), the color gradients are scaled to  
848 the maximum permissible biomass per grid node (see Supplementary Methods). For phages,  
849 the black color gradient is scaled to the maximum phage concentration in this run of the  
850 simulation. Any phages that diffuse away from the biofilm into the surrounding liquid are  
851 assumed to be advected out of the system in the next iteration cycle. Phages are introduced to  
852 the biofilm at 1.5 d. Phage infection proliferates along the biofilm front, causing biomass erosion  
853 and, in this example, complete eradication of the biofilm population. The simulation space is  
854 250  $\mu\text{m}$  long along its horizontal dimension.  
855  
856



857  
858  
859  
860  
861  
862  
863  
864  
865  
866  
867  
868  
869  
870  
871

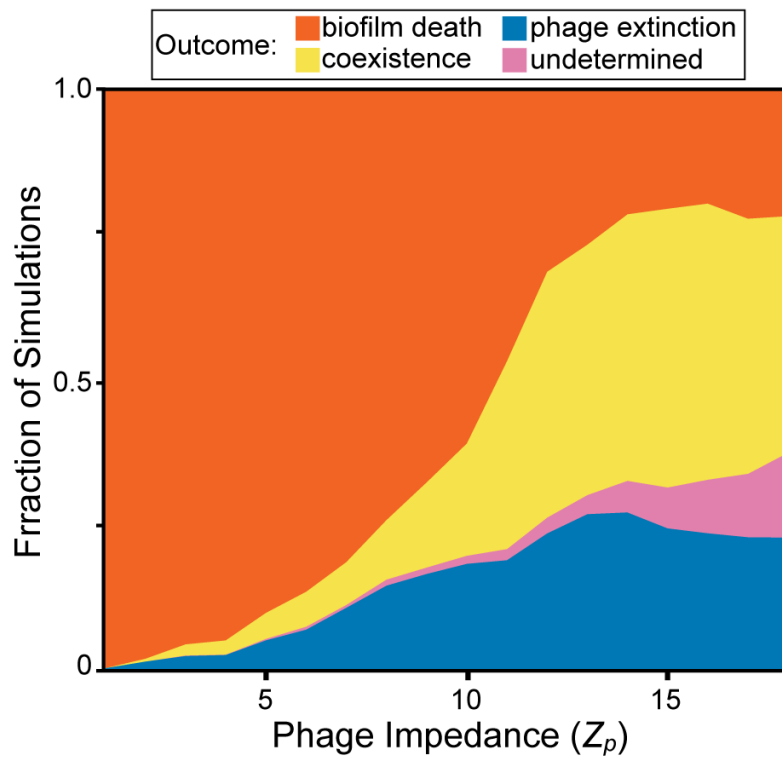
**Figure 2.** Population dynamics of biofilm-dwelling bacteria and phages for several example cases. For each example simulation, bacterial biomass is plotted in the thick dotted line (left axis), and phage counts are plotted in the thin solid line (right axis) (A) Biofilm death: phages rapidly proliferate and bacterial growth cannot compensate, resulting in clearance of the biofilm population (and halted phage proliferation thereafter). (B) Coexistence of bacteria and phages. We found two broad patterns of coexistence, one in which bacteria and phage populations remained at relative fixed population size (green lines), and one in which bacterial and phage populations oscillated as large biofilms clusters grew, sloughed, and re-grew repeatedly over time (black lines). (C) Phage extinction and biofilm survival. In many cases we found that phage populations extinguished while biofilms were relatively small, allowing the small population of remaining bacteria to grow unobstructed thereafter. Some of these cases involved phage population oscillations of large amplitude (black lines), while others did not (green lines).



872  
873

874 **Figure 3.** Steady states of biofilm-phage population dynamics as a function of nutrient  
875 availability, phage infection rate, and phage impedance. Each point in each heatmap  
876 summarizes >30 simulation runs, and shows the distribution of simulation outcomes. Phage  
877 extinction (biofilm survival) is denoted by blue, biofilm-phage coexistence is denoted by yellow,  
878 and biofilm death is denoted by orange. Each map is a parameter sweep of nutrient availability  
879 (~biofilm growth rate) on the vertical axis, and infection probability per phage-bacterium contact  
880 event on the horizontal axis. The sweep was performed for three values of  $Z_p$ , the phage  
881 impedance, where phage diffusivity within biofilm biofilms is equivalent to that in liquid for  $Z_p =$   
882 1 (panel A), and decreases with increasing  $Z_p$  (panels B and C). For  $Z_p = [10,15]$ , there are  
883 regions of stable coexistence (all-yellow points) and unstable coexistence (bi- and tri-modal  
884 points) between phages and bacteria. Traces of (D) bacterial biomass and (E) phage count are  
885 provided for one parameter combination at  $Z_p = 10$  (identified with a black box in panel B)  
886 corresponding to unstable phage-bacterial coexistence. We have highlighted one example each  
887 of phage extinction (blue), biofilm death (orange), and coexistence (yellow), which in this case  
888 is likely transient. In the highlighted traces, asterisks denote that the simulations were stopped  
889 because either phages or the bacterial biomass had declined to zero. This was done to increase  
890 the overall speed of the parallelized simulation framework. Simulations were designated  
891 "undetermined" if biofilms reached the ceiling of the simulation space before any of the other  
892 outcomes occurred (see main text).

893



894  
895  
896 **Figure 4.** The distribution of biofilm-phage population dynamic steady states as a function of  
897 increasing phage mobility impedance within the biofilm. Here we performed sweeps of nutrient  
898 and infection probability parameter space for values of phage impedance ( $Z_p$ ) ranging from 1-  
899 18. As the phage impedance parameter is increased, phage diffusion within the biofilm becomes  
900 slower relative to the surrounding liquid phase. The replication coverage was at least 6 runs for  
901 each combination of nutrient concentration, infection probability, and phage impedance, totaling  
902 96,000 simulations. Undetermined simulations are those in which biofilms reached the  
903 simulation height maximum before any of the other exit conditions occurred (see main text).